NASA/TM-20250006958

An Overview of Tire-Ground Contact Modeling Approaches for Surface Mobility Applications

Alexander Schepelmann, Colin M. Creager, Margaret P. Proctor, Kyle A. Johnson, and John R. Breckenridge
Glenn Research Center, Cleveland, Ohio

Asher Elmland
Jet Propulsion Laboratory, Pasadena, California

Paria Naghipour Ghezeljeh
HX5, LLC, Brook Park, Ohio

Heather A. Oravec
The University of Akron, Akron, Ohio

July 2025

NASA STI Program Report Series

Since its founding, NASA has been dedicated to the advancement of aeronautics and space science. The NASA scientific and technical information (STI) program plays a key part in helping NASA maintain this important role.

The NASA STI program operates under the auspices of the Agency Chief Information Officer. It collects, organizes, provides for archiving, and disseminates NASA's STI. The NASA STI program provides access to the NTRS Registered and its public interface, the NASA Technical Reports Server, thus providing one of the largest collections of aeronautical and space science STI in the world. Results are published in both non-NASA channels and by NASA in the NASA STI Report Series, which includes the following report types:

- TECHNICAL PUBLICATION.
  Reports of completed research or a major significant phase of research that present the results of NASA programs and include extensive data or theoretical analysis. Includes compilations of significant scientific and technical data and information deemed to be of continuing reference value. NASA counterpart of peer-reviewed formal professional papers but has less stringent limitations on manuscript length and extent of graphic presentations.

- TECHNICAL MEMORANDUM.
  Scientific and technical findings that are preliminary or of specialized interest, e.g., quick release reports, working papers, and bibliographies that contain minimal annotation. Does not contain extensive analysis.

- CONTRACTOR REPORT.
  Scientific and technical findings by NASA-sponsored contractors and grantees.

- CONFERENCE PUBLICATION.
  Collected papers from scientific and technical conferences, symposia, seminars, or other meetings sponsored or cosponsored by NASA.

- SPECIAL PUBLICATION.
  Scientific, technical, or historical information from NASA programs, projects, and missions, often concerned with subjects having substantial public interest.

- TECHNICAL TRANSLATION.
  English-language translations of foreign scientific and technical material pertinent to NASA's mission.

Specialized services also include organizing and publishing research results, distributing specialized research announcements and feeds, providing information desk and personal search support, and enabling data exchange services.

For more information about the NASA STI program, see the following:

- Access the NASA STI program home page at http://www.sti.nasa.gov

NASA/TM-20250006958

An Overview of Tire-Ground Contact Modeling Approaches for Surface Mobility Applications

Alexander Schepelmann, Colin M. Creager, Margaret P. Proctor, Kyle A. Johnson, and John R. Breckenridge
Glenn Research Center, Cleveland, Ohio

Asher Elmland
Jet Propulsion Laboratory, Pasadena, California

Paria Naghipour Ghezeljeh
HX5, LLC, Brook Park, Ohio

Heather A. Oravec
The University of Akron, Akron, Ohio

National Aeronautics and
Space Administration

Glenn Research Center
Cleveland, Ohio 44135

July 2025

Trade names and trademarks are used in this report for identification only. Their usage does not constitute an official endorsement, either expressed or implied, by the National Aeronautics and Space Administration.

Level of Review: This material has been technically reviewed by technical management.

This report is available in electronic form at https://www.sti.nasa.gov/ and https://ntrs.nasa.gov/

NASA STI Program/Mail Stop 050
NASA Langley Research Center
Hampton, VA 23681-2199

Abstract

Wheels and tires serve as the critical interface between vehicles and the ground, enabling traction, force transmission, and ultimately mobility. As planetary exploration systems adopt increasingly complex wheel and tire designs, look to explore increasingly extreme terrains, and adopt increasingly aggressive performance requirements, physics-based modeling has become essential for both designing these mechanisms and predicting performance under conditions that are difficult or impractical to replicate experimentally, such as reduced gravity. This paper provides a high-level overview of commonly used modeling approaches for simulating tire-ground interaction, including those currently employed or under development at NASA Glenn Research Center, NASA Johnson Space Center, and the Jet Propulsion Laboratory. The paper first categorizes modeling techniques based on their fidelity and underlying assumptions. It then discusses the applications, benefits, and limitations of each approach, highlighting current knowledge gaps and modeling challenges. Finally, the paper outlines ongoing and future work aimed at addressing these limitations, including initial results from automated soil preparation experiments that support the generation of consistent physical test data and the development of terramechanics simulations for evaluating and comparing model fidelity.

1 Introduction

Wheels and tires are the primary interface between vehicles and the ground, transmitting forces and enabling mobility. Throughout history, wheel and tire design has evolved from simple wooden discs to sophisticated systems featuring intricate tread patterns and other technologies to achieve better traction, stability, and energy efficiency depending on a vehicle's mobility goals. As this complexity has increased, modeling approaches have become essential for creating and optimizing wheel and tire designs.

Historically, empirical models were used to characterize contact between tires and the ground, relying on experimental data and empirically derived relationships.[1] With the advancement of computational power and engineering knowledge, numerical models have more recently emerged as powerful tools for tire-ground contact analysis. These models can provide detailed insights into the complex interactions between tires and the ground, enabling engineers to optimize vehicle performance and other mobility metrics.

[1]The terms "wheel" and "tire" are often used interchangeably. In this paper, a "wheel" refers to a rotating structure that converts torque into thrust, while a "tire" refers to the component on the wheel that interacts with and conforms to the ground. In most terrestrial applications, the distinction is clear, with the tire being the rubber, air-filled portion. However, for non-pneumatic planetary tires, this distinction is less defined. Therefore, the term "tire" will primarily be used to refer to the entire structure, as the focus of this paper is on ground interaction. However, since "wheel" is still commonly used in the field to describe this structure, both terms will appear throughout the paper.

The selection of a tire-ground modeling approach depends on various factors. Complex dynamic behavior, such as wheel slip and deformation, necessitates models that capture these phenomena accurately. Conversely, models designed for real-time applications or embedded systems require computational efficiency. Additionally, the availability of computational resources, which limit the complexity of models that can be employed, must also be considered when selecting a tire-ground modeling approach. By carefully considering these constraints, engineers can tailor their modeling approach to specific applications and achieve desired results.

This paper presents a high-level overview of commonly used tire-ground contact modeling approaches, including ones in-use and under development at NASA Glenn Research Center, NASA Johnson Space Center, and the Jet Propulsion Laboratory. These modeling approaches can be divided into three primary categories: *classical terramechanics* that rely on semi-empirical modeling, where various aspects of wheel-ground contact interaction are captured by combining experimental data with theoretical principles; *numerical models* where ground particles are modeled based on physical relationships either as a continuum or at the individual particle level that then interact with simulated wheel geometry; and *empirical approaches* that rely on physical testing to capture phenomena for specific, one-off, complex interactions where model development is time or cost prohibitive.

The paper begins by introducing the performance metrics used to quantify tire performance on granular media. Next the various modeling approaches across a range of fidelities are outlined with their key features and theoretical foundations. It then examines the applications and limitations of each approach, identifying current knowledge gaps and modeling challenges. This is followed by a summary of ongoing efforts to address these limitations, including soil characterization and simulation comparison work currently underway. The paper concludes with a discussion of planned future directions aimed at advancing modeling capabilities to support next-generation planetary mobility systems.

2 Mobility Metrics in Granular Terrain

To evaluate and compare the performance of different modeling approaches, it is first necessary to establish a common basis for assessing wheel mobility in granular media. This section introduces key performance metrics derived from standard wheel-soil interaction tests, which serve as important reference points for validating simulations and guiding model development throughout the remainder of this paper.

One widely used method for quantifying wheel performance is the single-wheel drawbar pull test [7]. This controlled experiment provides a repeatable means of assessing a wheel's traction, sinkage, and overall behavior when traversing loose soil. In the test setup, a single wheel is either driven or towed across a prepared soil bed while instrumented with sensors to capture forces and moments in all directions. The wheel is allowed to sink freely under a prescribed normal load, simulating realistic vehicle-terrain interaction conditions. By varying the wheel's slip ratio, which is further discussed in Section 3.2, researchers can systematically assess traction performance across a range of conditions.

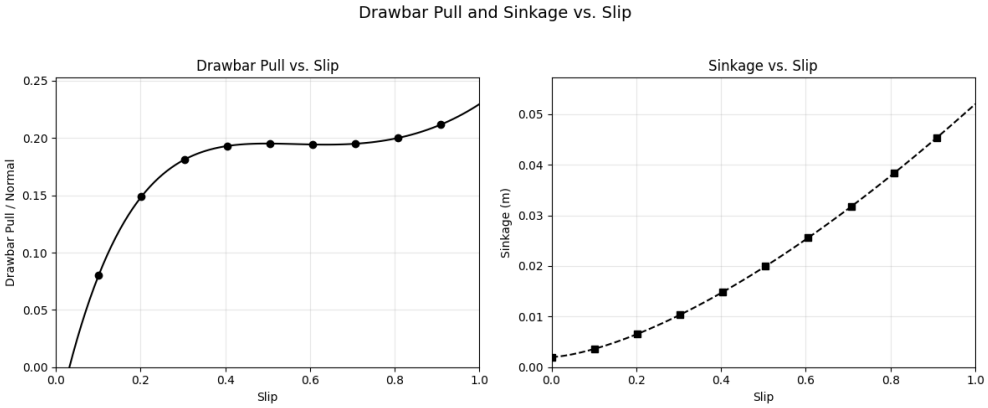

Figure 1. Example drawbar pull vs slip (left) and sinkage vs slip (right) curves.

Key outputs from this test include the normalized drawbar pull (longitudinal traction force divided by normal load) and incremental sinkage as a function of slip, examples of which are shown in Figure 1. These metrics, further discussed in Section 3.2, collectively define a performance envelope for the wheel under test and are used to evaluate traction capability, resistance to sinkage, and the likelihood of mobility degradation in soft terrain. Full six-axis force and moment measurements also provide insight into lateral slip, yaw moments, and terrain-induced asymmetries. These data are not only valuable for analyzing wheel designs but also play a critical role in calibrating and validating terramechanics simulation tools. As such, this performance framework provides essential context for interpreting the capabilities and limitations of the various modeling approaches discussed in subsequent sections.

3 Classical Terramechanics (Semi-Empirical Models)

Classical terramechanics approaches rely on semi-empirical modeling, where experimental data is combined with theoretical principles to create a mathematical description of various wheel-ground interaction phenomena. These approaches are useful for capturing specific phenomena that can then be applied to situations with similar conditions of the experiments that were used to create them. While generally having lower fidelity than numerical and empirical modeling approaches, semi-empirical models are easier to compute, making it possible to apply them in simulations that require real-time calculations or human-in-the-loop interaction, and are more generalizable than empirical relationships constructed to capture the dynamics of a specific test case. Details of various commonly used semi-empirical modeling approaches for mobility applications are described in the following sections, though the list is nowhere near exhaustive. Refer to [12] for a more comprehensive compilation of semi-empirical terramechanics models.

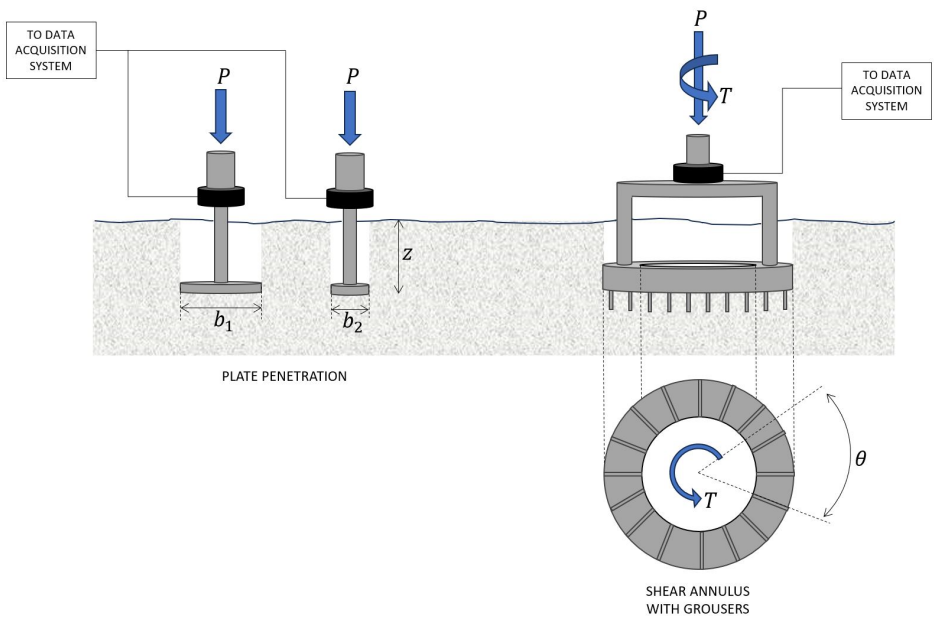

Figure 2. A typical bevameter test device [38].

3.1 Bekker, Wong, Janosi, and Hanamoto Models

The foundation of terrain-vehicle system interaction models relies on semi-empirical methods to obtain vertical and horizontal stress-strain relationships. From these relationships the resistance, thrust, and required torque can be approximated to evaluate vehicle design and performance.

There is only one test instrument that is configured to evaluate both the vertical and horizontal stress-strain relationships of the terrain. This instrument is called the bevameter, short for Bekker-Value-Meter, formally developed by M.G. Bekker in the 1950's (Fig. 2). This device was originally designed for soil measurement by the US Army Tank Automotive Command and is used to perform both the plate-sinkage and annular shear tests required to determine the vertical and horizontal stress-strain relationships of the terrain, respectively. During a plate-sinkage test, a rectangular or circular plate that matches the contact area of the vehicle running-gear is pushed vertically into the terrain with a constant rate of penetration. The applied force and resulting sinkage are measured and used to determine the vertical stress-strain relationship. During a shear test, an annulus with normal pressure similar to that of the wheel load is used to simulate the shearing action of the vehicle running gear, by rotating on the terrain surface at a constant rate. The applied torque and resulting angular displacement are measured and used to determine the horizontal stress-strain relationship.

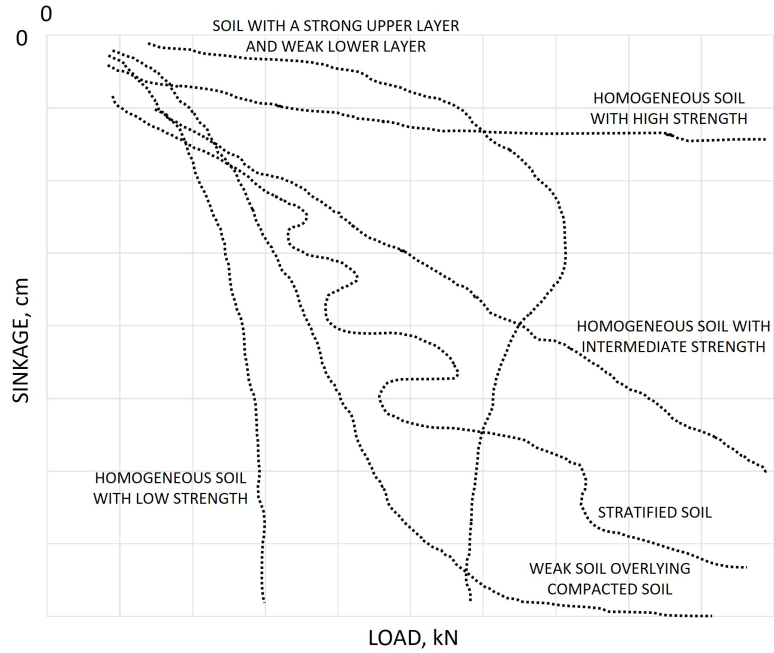

Figure 3. Typical load-sinkage curves for various types of terrain [4].

3.1.1 Vertical Stress-Strain Relationship

The vertical stress-strain relationship of the terrain, otherwise denoted as the "pressure-sinkage relationship," has taken several forms over the years [3][4][5][9][11][27]. The most well-known and generally accepted form was derived by M.G. Bekker and is shown in Equation 1. This relationship is used to determine the depth a wheel will sink into the ground under load and ultimately relates to the resistance (e.g., bulldozing) the wheel will encounter while driving [3][4]. The general concept behind Bekker's theory is that the normal stress beneath a wheel at a given depth is equivalent to that obtained in a plate-sinkage test at the same depth. In this equation, k_c and k_ϕ are empirically derived moduli of deformation which are dependent on the soil properties cohesion and friction angle, respectively, and are independent of plate shape and size. The parameter n is an empirically derived value dependent on the soil type and defines the shape of the load-penetration curve (refer to Fig. 3). The smaller dimension of the rectangular wheel ground contact patch or radius of the circular plate is represented by the parameter b. Pressure-sinkage curves for various types of terrain are shown in Figure 3.

$$p = (\frac{k_c}{b} + k_\phi)z^n \tag{1}$$

Here,

p = pressure
k_c = modulus of deformation with respect to soil cohesion

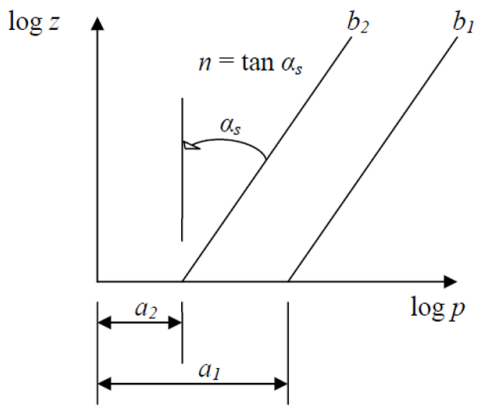

Figure 4. Resulting parallel lines from two plate-sinkage tests where a_1 and a_2 represent the pressures corresponding to the sinkage of $z = 1$ for each plate [36][38].

k_ϕ = modulus of deformation with respect to soil friction angle
b = the smaller dimension of the rectangular loading area or the radius of a circular plate
z = soil depth or sinkage, and
n = the empirical soil value which defines the shape of the penetration curve.

The plate-sinkage prediction method includes: 1.) running a minimum of two plate-sinkage tests with different sized plates in the same terrain to determine the vertical stress-strain relationship; 2.) calculating the empirical terrain parameters via curve-fitting techniques applied to the resulting pressure-sinkage curves from step 1; and 3.) predicting the pressure-sinkage characteristics of other different sized wheels (or tracks) by applying the parameters to the prediction equations. It should be noted that more than two tests or tests with more than two plates provides additional data and thus more accurate terrain parameters [21].

From a two-plate test, each test produces a pressure-sinkage curve, which on a log-log scale can be written as:

$$\log p_i = \log[k_c/b_i + k_\phi] + n \log z. \tag{2}$$

Here, p_i and b_i are dependent on the different plates (i) used in the load-penetration tests. For each plate, this relationship ideally defines a parallel line (Fig. 4) from which the parameters k_c, k_ϕ, and n can easily be determined [36][38].

Wong imposed a step-by-step weighted least squares method to obtain unique terrain parameters as well as a method for defining the error or "goodness-of-fit" between the experimental and theoretical data [36][38]. This method derives the best-fitted values of the pressure-sinkage terrain parameters to minimize the following function, F, using the weighting factor p^2,

$$F = \sum p^2 \left[\ln p - \ln\left(k_c/b + k_\phi\right) - n \ln z\right]^2. \tag{3}$$

To minimize Equation 3, the partial derivative of the function with respect to n and k_{eq}, where $k_{eq} = ({}^{k_c}/_{b} + k_\phi)$, is determined and set equal to zero. This leads to the following equations:

$$n = \frac{\sum p^2 \sum p^2 \ln p \ln z - \sum p^2 \ln p \sum p^2 \ln z}{\sum p^2 \sum p^2 (\ln z)^2 - (\sum p^2 \ln z)^2} \tag{4}$$

$$\ln k_{eq} = \frac{\sum p^2 \ln p - n \sum p^2 \ln z}{\sum p^2}. \tag{5}$$

A unique n value is usually obtained for each plate size, so it is necessary to average the values when calculating the natural logarithm of k_{eq} in Equation 5. Similarly, there will be two k_{eq} values, one for each plate. The following equations can be used to determine k_c and k_ϕ:

$$k_c = \frac{(k_{eq})_{b_1} - (k_{eq})_{b_2}}{b_2 - b_1} b_1 b_2 \tag{6}$$

$$k_\phi = (k_{eq})_{b_1} - \left[\frac{(k_{eq})_{b_1} - (k_{eq})_{b_2}}{b_2 - b_1}\right] b_2. \tag{7}$$

It is important to note, when following this analysis, that the value for k_c is commonly negative for dry granular soils [9].

To determine the goodness-of-fit, the ratio of the root-mean-square error to the mean value of the pressure in Equation 8 is applied [36]:

$$\varepsilon = \frac{\sqrt{\frac{\sum (p_m - p_c)^2}{(N-2)}}}{\sum {}^{p_m}/_{N}}. \tag{8}$$

Here, p_m is the experimental value of pressure and p_c is the theoretical value from Equation 1. N is the number of points used when curve-fitting. A perfect fit is defined as $\varepsilon = 0$. Typical measured and theoretical load-sinkage curves for dry granular terrain are shown in Figure 5 and typical Bekker parameters for various types of terrain are shown in Table 1. Unfortunately, no true Bekker parameters exist for lunar regolith, since that data would have needed to be collected in-situ on the lunar surface. During Apollo, parameters were estimated based on Surveyor data to support Apollo simulations [6], but these should only be considered rough estimates and do not encompass the entire range of lunar regolith parameter possibilities. Additionally, little data exists on lunar soil at the South Pole. Bekker parameters are also dependent on wheel size and loading conditions. Future work is needed to identify an appropriate range of Bekker parameters for simulations of vehicles operating at the lunar South Pole.

Table 1. Typical Bekker values for various terrain types and moisture content [37].

Terrain Type	**Moisture Content (%)**	n	k_c **(kN/m^{n+1})**	k_ϕ **(kN/m^{n+2})**	c **(kPa)**	ϕ **(deg)**
Dry Sand	0	1.1	0.99	1528.43	1.04	28
Sandy Loam	15	0.7	5.27	1515.04	1.72	29
	22	0.2	2.56	43.12	1.38	38
	11	0.9	52.53	11127.97	4.83	20
	23	0.4	11.42	808.96	9.65	35
	26	0.3	2.79	141.11	13.79	22
	32	0.5	0.77	51.91	5.17	11
Clayey Soil	38	0.5	13.19	692.15	4.14	13
	55	0.7	16.03	1262.53	2.07	10
Heavy Clay	25	0.13	12.70	1555.95	69.95	34
	40	0.11	1.84	103.27	20.69	6
Lean Clay	22	0.2	16.43	1724.69	68.95	20
	32	0.15	1.52	119.61	13.79	11
LETE Sand	–	0.79	102	5301	1.3	31.1
Upland Sandy Loam	51	1.10	74.6	2080	3.3	33.7
Rubicon Sandy Loam	43	0.66	6.9	752	3.7	29.8
North Gower Clayey Loam	46	0.73	41.6	2471	6.1	26.6
Grenville Loam	24	1.01	0.06	5880	3.1	29.8
Snow (US)	–	1.6	4.37	196.72	1.03	19.7
	–	1.6	2.49	245.90	0.62	23.2
Snow (Sweden)	–	1.44	10.55	66.08	6	20.7
GRC-1 (ρ = 1.67 g/cc, RD = 27.3%)	–	1.234	4009.91	-22368.57	–	33.7
GRC-3 (prepared to loose condition)	–	1.0	23.2	606.7	0.13	36.7

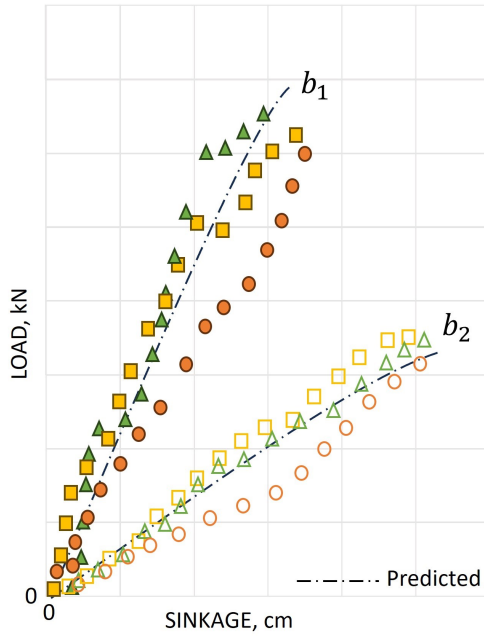

Figure 5. Example of measured and calculated load-sinkage curves for dry granular terrain following the Bekker-Wong method [36][38].

3.1.2 Horizontal Stress-Strain Relationship

The horizontal stress-strain relationship or the shear stress-shear displacement relationship, shown in Equation 9, was developed by Janosi and Hanamoto in 1961 [17]. This equation is used to determine the amount of traction that a wheel will generate and how easily it will progress through terrain and surmount obstacles when driven. In Equation 9, c and ϕ are the cohesion and angle of internal friction of the terrain, respectively. K is the shear deformation modulus which is the magnitude of the shear displacement required to develop the maximum shear stress.

$$\tau = (c + \sigma \tan \phi)\left(1 - e^{-\frac{j}{K}}\right) \tag{9}$$

Here,

τ = shear stress
c = soil cohesion
σ = vehicle weight
ϕ = soil friction angle
j = shear displacement, and
K = the shear deformation modulus of the soil.

The shear stress-shear displacement prediction method includes: 1.) conducting a minimum of five to seven annular shear bevameter tests in the same terrain, each

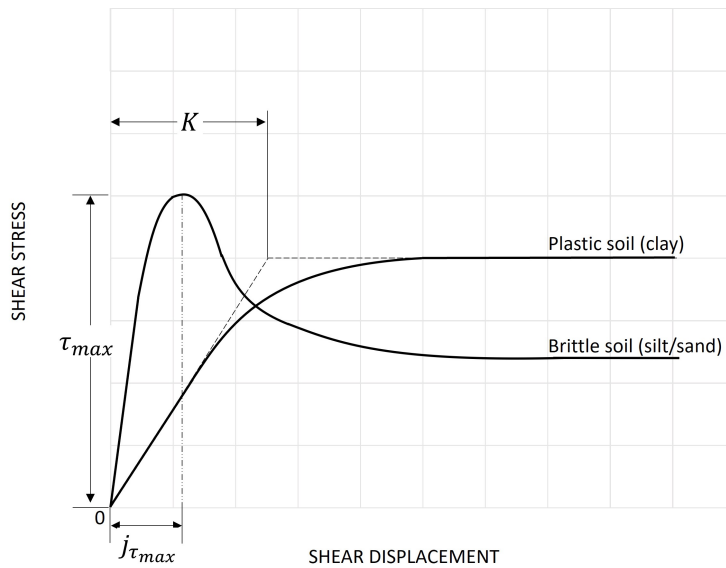

Figure 6. Typical shear stress-displacement responses for brittle and plastic terrain types [36].

with a different applied normal load [4]; 2.) applying curve-fitting techniques to determine the parameters of the prediction equation; and 3.) applying the parameters to the prediction equation to determine the theoretical shear stress-shear displacement characteristics of similar objects. Typical horizontal stress-strain relationships for plastic and brittle soils (e.g., clays and silts/sands, respectively) are shown in Figure 6.

Similar to the plate-sinkage prediction method, Wong developed a simple and reliable data processing methodology to obtain the horizontal stress-strain terrain parameters [36]. A weighted least squares method is used to determine the best value of K to minimize the error in the curve fit. Wong also developed a means to evaluate goodness-of-fit of the theoretical curve compared to the experimental curve. Wong's method begins with taking the natural logarithm of both sides of Equation 9 and results in the following equation:

$$F = \sum \left(1 - \frac{\tau}{\tau_{max}}\right)^2 \left[\ln\left(1 - \frac{\tau}{\tau_{max}}\right) + \frac{j}{K}\right]^2. \tag{10}$$

Here, the weighting factor is $\left(1 - \frac{\tau}{\tau_{max}}\right)^2$. This equation must be minimized to determine the best value of K by taking the first partial derivative of the function with respect to K and setting it equal to zero. This results in

$$K = -\frac{\sum \left(1 - \tau/\tau_{max}\right)^2 j^2}{\sum \left(1 - \tau/\tau_{max}\right)^2 j \left[\ln\left(1 - \tau/\tau_{max}\right)\right]}. \tag{11}$$

The goodness-of-fit is determined through

$$\varepsilon = \frac{\sqrt{\frac{\sum(\tau_m - \tau_c)^2}{(N-2)}}}{\sum \tau_m / N} \tag{12}$$

where τ_m is the measured shear stress and τ_c is the theoretical shear stress using Equation 9. The curve-fit is defined as a perfect fit when $\varepsilon = 0$. Typical shear stress-shear displacement curves are shown in Figure 7 for a sandy terrain. Refer to Table 1 for typical c and ϕ terrain values.

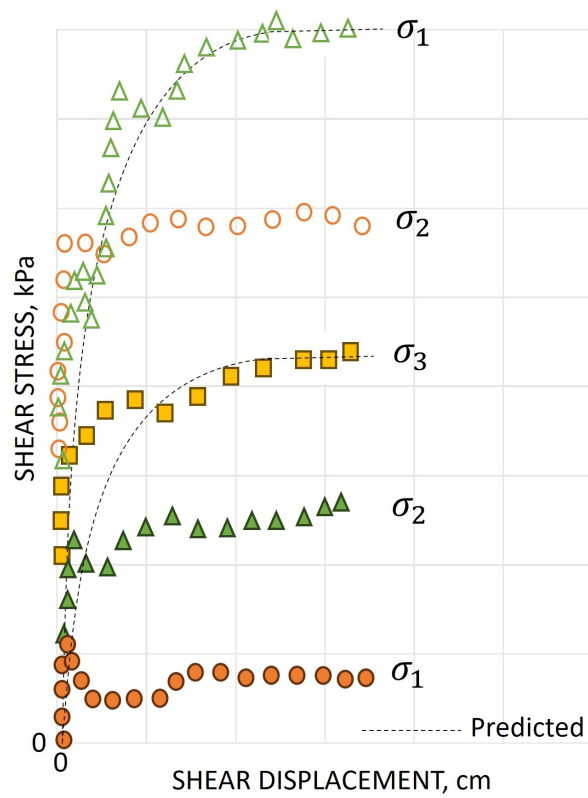

Figure 7. Typical horizontal stress-displacement responses for sandy terrain. [36].

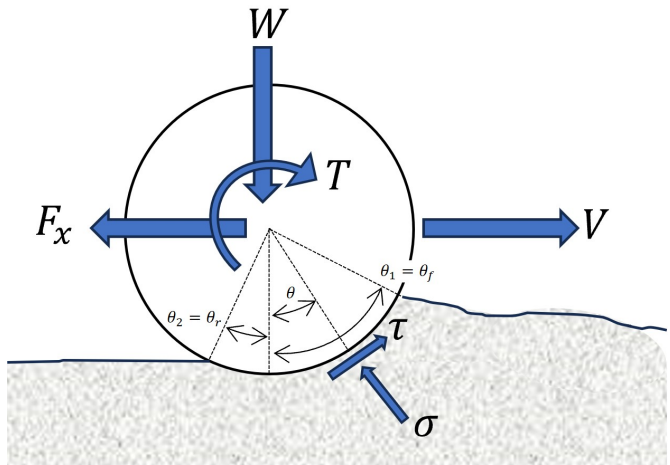

Figure 8. Diagram of the forces (F_x = drawbar pull, W = wheel load), torque (T), and stresses (τ = shear stress, σ = radial stress, both acting at the wheel soil interface) acting on a rigid wheel driving over soft terrain (V = forward velocity of the wheel) [39].

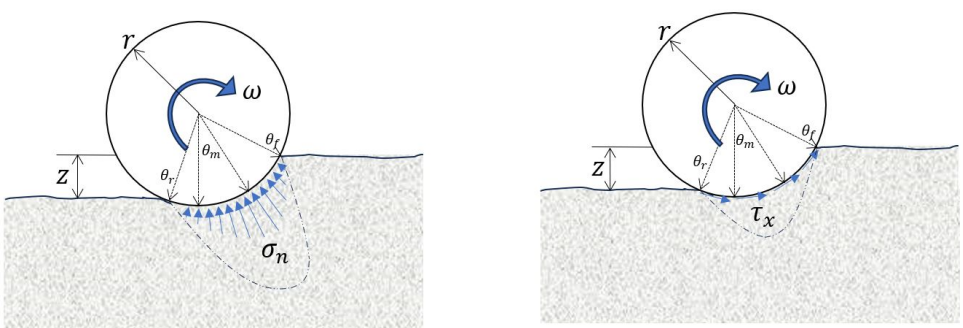

Figure 9. Normal (left, σ_n) and tangential (right, τ_x) stress distribution on a rigid wheel (ω = angular wheel velocity).

Table 2. Typical values for c_1 and c_2 for various types of sand [39].

Terrain Type	**Angle of Internal Friction ϕ**	**Cohesion c (lb/in.^{2})**	**Density (lb/in.^{3})**	c_1	c_2
Compact Sand	33.3^o	0.10	0.0575	0.43	0.32
Loose Sand	31.1^o	0.12	0.048	0.18	0.32
Sand	36.0^o	0.10	0.0617	0.285	0.32
Dry Sand	24.0^o	–	–	0.38	0.41

3.2 Wong and Reece Model

Another notable semi-empirical model, based upon Bekker's vertical stress-strain relation and Janosi-Hanamoto's horizontal stress-strain relation, is the wheel-terrain model derived by Wong for rigid wheels on soft terrain [1][39]. The wheel torque, thrust, and sinkage are derived by estimating stress distributions along the wheel-terrain interface. In this two-dimensional model (ignoring out of plane motion), the stress distribution under a wheel are divided into the normal and tangential stress (refer to Figures 8 and 9).

The normal stress for a wheel driving along a terrain interface can be represented by the following equations [1]:

$$\sigma = \sigma_1 = \left(\frac{k_c}{b} + k_\phi\right) z_1^n \quad \text{for} \quad \theta_m < \theta < \theta_1 \tag{13}$$

$$\sigma = \sigma_2 = \left(\frac{k_c}{b} + k_\phi\right) z_2^n \quad \text{for} \quad \theta_2 < \theta < \theta_m \tag{14}$$

Here,

σ_1 = normal stress from the point of soil entry to the maximum normal stress
σ_2 = normal stress from the point of maximum normal stress to the point of soil exit
$\left(\frac{k_c}{b} + k_\phi\right) z_i^n$ = Bekker's pressure-sinkage relationship
$\theta_1 = \theta_f$ = the angle of soil entry
θ_m = the angle at the point of maximum normal stress, and
$\theta_2 = \theta_r$ = the angle of soil exit.

Here, $z_1 = r\left(\cos\theta - \cos\theta_1\right)$ and $z_2 = r\left(\cos\left(\theta_1 - \frac{\theta-\theta_2}{\theta_m-\theta_2}\right)(\theta_2 - \theta_m)\right) - \cos\theta_2$. r is the radius of the rigid wheel. The angle where maximum normal stress occurs is calculated as

$$\theta_m = \left(c_1 + c_2 s\right)\theta_1 \tag{15}$$

where c_1 and c_2 are empirically derived parameters for determining the relative position of maximum radial stress and s is the wheel slip. Here, slip is

$$s = 1 - V/r(\omega), \tag{16}$$

where V is the actual translational speed of the wheel, r is the radius of the wheel, and ω is the angular speed of the wheel. The theoretical forward translation of the wheel is equivalent to $r\omega$. Coefficients c_1 and c_2 for sand are shown in Table 2.

The shear stress in the horizontal direction is what drives the tractive performance of the wheel. Recall from [17] that Equation 9 defines the shear stress (τ)

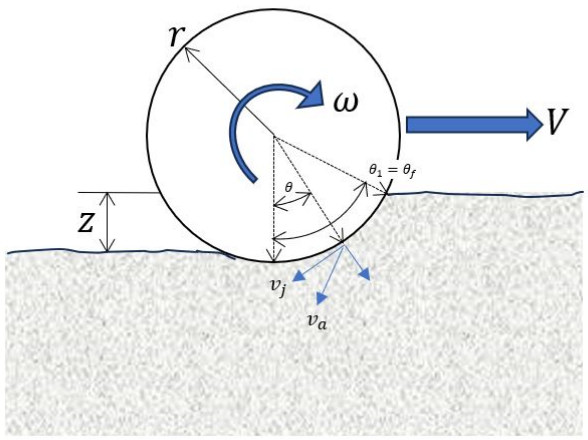

Figure 10. Schematic of shear deformation beneath a rigid wheel [39]. v_j is the slip velocity of the wheel and v_a is the absolute velocity of the wheel.

as a function of the normal stress (σ), various semi-empirical soil parameters (c, ϕ, and K), and measured shear displacement (j). To determine the tangential stress distribution along the wheel, the shear displacement is needed. This can be determined by calculating the slip velocity (v_j) of the wheel relative to the soil (refer to Figures 9-10, [39]):

$$v_j = r\omega\left[1 - (1 - i)\cos\theta\right] \tag{17}$$

where r is the radius of the wheel, ω is the rotational velocity of the wheel, i is the slip value and θ is the angle of rotation. From Equation 17, the shear deformation, j, can be calculated as

$$\begin{aligned} j &= \int_0^t v_j dt = \int_0^{\theta_1} r\omega\left[1 - (1 - i)\cos\theta\right]\frac{d\theta}{\omega} \\ &= r\left[(\theta_1 - \theta) - (1 - i)\left(\sin\theta_1 - \sin\theta\right)\right]. \end{aligned} \tag{18}$$

Substituting Equation 18 into Equation 9, the shear stress around the wheel can be calculated as

$$\tau(\theta) = (c + \sigma(\theta)\tan\phi)\left(1 - e^{-\frac{r[(\theta_1-\theta)-(1-i)(\sin\theta_1-\sin\theta)]}{K}}\right) \tag{19}$$

where σ_1 and σ_2 can be determined using Equations 13 and 14 for the soil entry (front) and exit (rear) regions, respectively.

If the soil parameters, wheel dimensions, parameters for determining the relative position of maximum radial stress, and wheel load are known, the wheel performance can be predicted. To predict the wheel performance, the following equations have been derived in [39]. For wheel thrust (F_T) the sum of all shear force components in the direction of forward motion is calculated as

$$F_T = br \int_{\theta_r}^{\theta_f} \tau \cos\theta d\theta, \tag{20}$$

compaction resistance (R_c), resulting from static and dynamic (slip sinkage) wheel sinkage is calculated as the sum of all normal force components resisting forward motion

$$R_c = br \int_{\theta_r}^{\theta_f} \sigma \sin\theta d\theta, \tag{21}$$

and drawbar pull force (F_x) is determined as the difference between the thrust force and the resistance force (the net horizontal force) which can either act to accelerate the wheel or provide a towing force at the vehicle axle:

$$F_x = F_T - R_c. \tag{22}$$

Finally, driving torque, T, can be evaluated by integrating the shear stress around the wheel at the soil interface:

$$T = br^2 \int_{\theta_r}^{\theta_f} \tau d\theta. \tag{23}$$

4 Numerical Models

Semi-empirical models are computationally efficient and can capture certain aspects of rigid wheel-ground interaction. However, their usefulness is limited when dealing with complex terrain or modeling the dynamics of compliant wheel-ground interaction. In such cases, numerical models are more appropriate. Although numerical methods are often too computationally demanding for real-time applications, they are crucial for accurately modeling complex wheel-ground interactions, aggressive vehicle dynamics, and vehicles with compliant wheels.

This section offers an overview of various numerical modeling techniques currently in use or under investigation at NASA's Glenn Research Center and Johnson Space Center for mobility research. Since these models are more complex than the semi-empirical approaches discussed in the previous section, and the specific numerical methods often depend on the simulation software used, this overview focuses on different types of numerical models rather than providing detailed implementation

steps. Readers are strongly encouraged to familiarize themselves with the implementation details of their chosen software package to fully understand its benefits, capabilities, and limitations. At NASA, numerical models have been used to simulate the loading response in compliant Spring Tires [22], as well as the interaction between soil and thin-walled structures [22]. Modeling the interaction between soil and compliant tires has been investigated at Glenn Research Center but further development is still needed. Therefore, each type of numerical model described below will be discussed within this context.

4.0.1 Compliant Tire Modeling

Non-rigid deformable tires are complex anisotropic structures that are challenging to model. Numerical tire modeling using Finite Element Modeling (FEM) has been increasingly used in recent years to investigate and better understand tire-terrain interactions. Accurately capturing tire deformation is critical, as it affects the sinkage and guides the entire design process. The use of 3D models is essential to capture the relevant mechanisms and obtain meaningful results that represent the true physics of the system. Simplified 2D models or section modeling and extrapolation can lead to misleading design choices, especially if the tire is made of novel materials like Shape Memory Alloys (SMAs).

A recent paper by Naghipour *et al.* provides a comprehensive summary of the build, analysis, validation, and design process of deformable Spring Tires made of SMAs under the Mars Sample Return program at NASA Glenn Research Center (GRC) [23]. The study aimed to evaluate the structural design of the deformable SMA tires through numerical analysis and sensitivity studies. Design variables were varied to analyze their impact on the tire's global load-displacement response, and a detailed investigation of the three-dimensional stress states enhanced understanding of local changes during global tire deformation. The results demonstrated that a robust numerical model with good predictive capabilities, combined with a carefully conducted sensitivity study, can reduce the number of design iterations needed to achieve the desired tire performance. This, in turn, reduces manufacturing time, labor, and testing costs.

While tires vary in complexity based on their construction, no other studies in the current literature apart from [23] have addressed in-depth modeling and analysis of deformable tires made of fully nonlinear material systems. Expanding this modeling capability to account for the interaction between the tire and soil was investigated; however, that capability does not currently exist and requires further development.

4.0.2 Continuum Modeling

Traditionally, soils have been modeled using empirical and semi-empirical equations due to the complexity of the task. However, recent advances have enabled the use of physics-based continuum mechanics frameworks such as FEM and Smoothed Particle Hydrodynamics (SPH) for terrain modeling. These model granular media as a continuum and are therefore useful for estimating large scale responses generated by tire terrain interaction. These approaches require material constitutive laws that

describe the relationship between stress and strain, which are essential for accurately simulating soil behavior.

No single soil constitutive model is universally applicable for all types of soil in every scenario. Therefore, researchers must select constitutive laws based on the specific features required for their simulations. Depending on the complexity of the model, the following factors may need to be defined: (a) yield surface, (b) hardening law, and (c) plastic flow rule. The yield surface defines the limits within which the soil behaves elastically. The hardening law dictates how the yield surface evolves once plastic deformation begins, typically as a function of strain. The plastic flow rule defines the direction of plastic deformation, with non-associative flow rules requiring the user to input the plastic potential separately.

Popular FEM packages such as LS-Dyna, ABAQUS, and ANSYS include built-in soil constitutive models like Mohr-Coulomb, Drucker-Prager, Drucker-Prager Cap, and Cam-Clay. These models combine concepts such as volumetric deformation, consolidation behavior, stress history, and pore pressure evolution to predict soil behavior accurately. However, these highly accurate models require more computational resources, input data, and user effort.

Material characterization methods commonly applied to semi-empirical models are also applicable to continuum models. These include common geotechnical tests such as triaxial tests (to determine strength parameters), uniaxial compression tests (for stiffness parameters), and direct shear or ring shear tests (for stiffness and residual strength parameters). In-situ testing, such as Cone Penetrometer Testing (CPT), is also widely used to estimate material parameters in real-world conditions.

4.0.3 Discrete Element Modeling

The Discrete Element Method (DEM) is a widely-used computational approach for simulating the behavior of granular materials and their interactions with wheeled vehicles, particularly in challenging environments such as extraterrestrial surfaces. Originally developed by Cundall and Strack, DEM models granular systems by representing materials as a collection of discrete elements, typically particles of simple shapes like spheres or circles [8]. These elements interact with each other according to defined physical laws, such as contact forces and friction, allowing the method to capture complex dynamics like soil deformation and wheel-terrain interactions, including particle-tire interactions that may be important to capture dynamics of non-pneumatic mesh tires interacting with granular media [35].

At the core of DEM simulations is the process of tracking individual particles and their mutual interactions [8][35]. The method is governed by Newton's second law of motion, where all forces acting on each element, such as contact forces and gravitational forces, are summed to calculate accelerations, which are then integrated over time to obtain velocities and displacements. DEM primarily uses explicit integration techniques, such as the central difference method, which require very small time steps for numerical stability, especially when dealing with stiff materials or small particles. The contact between particles is typically modeled using linear spring or Hertz models for normal forces, and Mindlin-Deresiewicz models for tangential

forces, sometimes incorporating viscous damping to account for energy dissipation during collisions.

One of the key challenges in DEM simulations is the computational cost, particularly for systems with large numbers of particles. This cost stems from two primary factors: the small time steps required for stability and the computational intensity of detecting and managing collisions between particles. As a result, DEM simulations are often limited in scale, with typical simulations involving between 10^3 to 10^5 elements, far fewer than what would be required to model, for example, a cubic meter of real sand containing billions of particles. To reduce computational burden, particles in DEM simulations may also be larger than real-world counterparts being modeled. To address this, DEM has been accelerated using various parallel computing techniques, including CPU-based approaches with OpenMP and MPI for distributed memory systems, as well as GPU-based computing, which has gained popularity due to its efficiency in handling large-scale simulations [40].

Despite these advancements, simplifying assumptions are often made to reduce computational demands. For instance, spherical particles are widely used because they simplify the collision detection process and reduce simulation time, though this can sometimes compromise the accuracy of the model, particularly when dealing with irregularly shaped particles or complex terrain interactions. In some cases, more realistic particle shapes, such as ellipsoids, polygons, or clumps of multiple circles, are used, but this increases the complexity and computational load.

In the context of wheeled vehicle mobility on granular surfaces, DEM has proven to be a valuable tool for predicting how wheels interact with soil, providing insights into vehicle performance and terrain deformation [14][24][19][18][40]. DEM is capable of modeling complex phenomena such as slip, sinkage, and soil compaction, providing valuable insights into vehicle performance in off-road or extraterrestrial environments. However, the method's limitations, particularly in terms of computational scale and the reliance on simplified particle geometries, mean that researchers must carefully calibrate and validate their models using experimental data. Through such efforts, DEM continues to evolve, offering increasingly accurate and detailed simulations for understanding granular media and vehicle-terrain interactions in both terrestrial and extraterrestrial environments.

4.0.4 Modeling of Soil-Tire Interfaces

Modeling the tire-soil interface is crucial and remains one of the major gaps in the field. Depending on the modeling approach, two or more (up to millions) of bodies interact during contact, transmitting forces between them. In FEM-based tire-terrain models, surface-to-surface contacts are commonly used, while in FEM-SPH models, node-to-surface contact is employed. Contact algorithms are usually penalty-based to prevent the terrain and tire surfaces from penetrating each other. Tangential shear forces at the tire-soil interface are captured using friction laws, most commonly the Coulomb friction model.

The accuracy of friction and penalty models is essential, and they must be validated through friction calibration tests. However, limited experimental studies have focused on calibrating these models. For example, Papamichael and Vrettos [26]

Figure 11. The Apollo Lunar Roving Vehicle Tire [2].

conducted direct shear tests between tires and soil to model soil-terrain interaction, while Shoop [33] suggested traction and braking tests to determine normal friction coefficients at the tire-terrain interface. Beyond these studies, few experimental investigations exist to validate FEM-based tire-terrain models. Friction coefficients can significantly impact simulation results, especially in quasi-static scenarios. Addressing this gap is crucial before implementing large-scale numerical models that integrate all the elements, including tires, terrain, and the tire-terrain interface.

To supplement the deformable tire model during the Mars Sample Return project, a preliminary soil model was developed at NASA Glenn Research Center utilizing SPH. The soil was characterized using the experiments previously conducted on pre-existing lunar soil data at GRC, which was then validated using cone penetrometer data in [25]. The methodology followed here was based on the author's prior experience with soil impact modeling [22]. To continue model development, soil and the deformable tire models should be combined into a holistic interacting simulation, which was not pursued at the time due to resource and schedule constraints.

5 Empirical Models

There may be instances where utilizing one of the modeling techniques mentioned above is either not feasible or not time and cost effective. While semi-empirical models are effective at capturing general dynamics, and capabilities of numerical modeling continues to advance rapidly, developing empirical relationships through testing may be quicker and sufficient for handling uncommon mobility scenarios, as these passively capture relevant factors including rock geometry, surface roughness, three-dimensional tire conformity around a rock, and tread features on a tire.

Empirical values established through testing can also account for multi-scale interactions, which have been found to be important for capturing performance of flexible wire-mesh tires. For example, in the case of the wire-mesh tires utilized on the Apollo Lunar Roving Vehicle (LRV) (Fig. 11), both bulk mechanical regolith properties and local interactions affected mobility. Specifically, it was observed that soil flow through the porous tire mesh impacted tire flotation [10][2]. The Bekker-Wong terramechanics model was used to predict the performance of this tire in granular soil; however the model assumed a constant pressure distribution in the footprint and could not account for soil flow through the mesh. Thus empirical testing was needed to determine the appropriate amount of tread coverage to reduce soil flow and minimize sinkage.

A previously implemented approach involves conducting laboratory tests at the component level (e.g., tires) to generate look-up tables for use in system-level simulations (e.g., rover). This method was applied during the design of the Mars Sample Return Fetch Rover, which featured four compliant SMA Spring Tires on a passive suspension. The Spring Tires were thoroughly characterized to provide parameters necessary for full system simulations, including data on tire deformation under load, friction on bedrock, torque and thrust over rocks, and the relationship between slip, sinkage, and tractive force. These tables enabled reliable system-level simulations to verify performance and power requirements without the need to model the complex tire-terrain interactions in detail.

Empirical relationships, while often tailored to specific mobility scenarios, can be integrated into system-level simulations, including real-time simulations, due to their mathematical simplicity. Below are examples of empirical data that can be used as parameters in these simulations:

1. **Soft soil traction.** Single-wheel tests performed in appropriate soil simulants can provide relationships between the tractive coefficient (net traction normalized by vertical load), slip, and sinkage. During a simulation, relevant wheel slip and sinkage values based on a vehicle's configuration (e.g. wheel loads, pose, slope angle) can be applied to predict overall vehicle performance.

2. **Bedrock/compacted ground friction.** Single-wheel tests on hard surfaces can determine friction coefficients. These coefficients can then be incorporated into the rover simulation to model interactions with bedrock or compacted ground.

3. **Tire stiffness/rolling resistance.** Load-deflection and rolling resistance tests on individual tires yield data that can be used to assess rover performance, including pose and power consumption, under various driving conditions.

4. **Rock traversal.** Single-wheel tests on rocks can measure tire torque, deformation, and thrust across different loading and rock configurations. This data helps predict the rover's performance when traversing rocky terrain.

6 Discussion

6.1 Best Practices and Lessons Learned: Bekker, Wong, Janosi, and Hamamoto Models

This section describes best practices and lessons learned for the soil models presented in Section 3.1. The accuracy of these semi-empirical models continues to be a challenging problem in terramechanics. These methods were originally developed for unconfined, homogeneous terrain, without imposed boundary conditions, though it can be argued that the soil over the depth affected by vehicle traffic is shallow enough to act as a homogeneous soil.

In addition, the experimental data from the plate-penetration tests rarely fits Equation 1 very well [36]. Similarly, the data from the shear tests does not perfectly align with Equation 9. Therefore, there is a lot of user manipulation involved in the data processing and curve-fitting techniques. A highly experienced investigator is necessary for proper interpretation, but it is important to understand that two different investigators would likely get two different solutions.

It should be noted that Equation 1 and Equation 9 are only able to predict accurately within the limitations of the bevameter test itself. More specifically, Equation 1 can only reliably predict the performance of wheels with a contact patch that is similar in size and shape to the plates used in the test [31]. Therefore, plate sizes should be selected that are similar in contact area of the wheel footprint. It should be noted that the shape of the penetrometer plate is not as critical as the size of plate, as smaller penetration plates are more sensitive to small changes in terrain consistency [13]. The larger the plate size the better. Additionally, the larger the difference between the two plate sizes the better such that the pressure-sinkage relationship for contact areas within the range of plate sizes used for testing can be predicted.

Similarly, the evaluation of the shear stress-shear displacement prediction equation parameters is not a trivial task. This relationship is intended for plastic-type soils (clays). Equation 2 is only able to predict accurately within the limitations of the annular shear bevameter test itself. The shear-stress-shear displacement relationship can only be predicted for vehicles with similar pressure range and similar contact area to the annular rings used in the bevameter tests. For vehicle mobility prediction, the larger the annular ring size and the larger the range of normal pressures, the better. They should be similar to the vehicle whose performance is in question. However, if the test is performed in the field where the terrain surface is not perfectly level, the annular ring size should be selected such that the entire surface area contacts the terrain. Additionally, a larger diameter annular ring will provide a larger horizontal shearing area for better linear approximations and ultimately more accurate values of cohesion and friction angle [4]. A ring with minimal difference in the inner and outer diameters will develop more uniform stress from the inner diameter to the outer diameter of the ring. The addition of grousers and spacing between grousers should also be considered in the design of the annular rings and be as similar as possible to the wheel design.

6.2 Best Practices and Lessons Learned: Wong and Reece Model

While the Wong-Reece model effectively predicts the performance of driven rigid wheels, there are several caveats that should be noted [39]. First, there is a relationship between the normal stress distribution on the wheel and the slip value. Generally, the normal stress shifts forward along the wheel-soil interface as the value of slip increases. Thus, it should be noted that motion resistance (dynamic sinkage) is a function of slip (slip-sinkage). Second, the process for determining the values of c_1 and c_2 is an empirical process. This can result in similar problems as when utilizing the bevameter, as the values are only as good as the test and multiple different values can possibly be obtained by different experimentalists. In addition, this model was developed for homogeneous soils and it is unknown how layered or inhomogeneous soils may affect the resulting predictions. One major limitation of this approach is that it was developed to model rigid cylindrical wheels. As a result, tire compliance and tread features, like grousers, which have major impacts on mobility performance, are not accounted for. Additional research is needed to apply these approaches to more complex tire geometries and mobility systems with tire compliance.

6.3 Best Practices and Lessons Learned: Numerical Models

Validating numerical models for tire-terrain interactions requires multiple levels of verification to ensure their accuracy. This includes validating the terrain material model, the tire model, and the interaction of the tire with deformable soil under both quasi-static and dynamic loads. Some validation studies are briefly discussed in this section.

First, when validating a deformable terrain model, it's crucial not to use the same tests employed for model characterization or parameterization, as this would result in re-calibration rather than validation. For example, if triaxial shear tests were used for terrain characterization, the validation should be conducted with different tests, such as Cone Penetration Tests [29]. Fortunately, the civil engineering field provides a wealth of experimental data on various terrains (soil, granular sand, etc.) that can be used for model validation.

Next, for validating tire models, structural-level tests are considered the gold standard, especially when dealing with novel materials. The tire material should be characterized before any structural analysis and kept consistent when testing different tire geometries. A commonly used structural test is the flat-plate compressive test, performed under both dynamic and static conditions [23]. Dynamic tests, like the drum-cleat test, which validate the first mode of vibration harmonics, have been explored in some studies, though they are less common than traditional structural experiments [30].

At this time, validation studies for tire-terrain interaction models are extremely limited, making this an important area for future experimental or numerical investigation. There may be situations where particle-to-particle or particle-to-tire interactions are critical, for example when soil particles flow through a mesh tire like the ones used on the Apollo LRV. These considerations have significant impacts

on how model parameters are selected and implemented. Additionally, modeling large-scale deformable tires is a non-trivial computational task in and of itself, which currently requires the use of finite element analysis (FEA) tools. Models that aim to simulate representative dynamics of these systems need to account for both tire compliance and granular tire-terrain interaction simultaneously. In cases where this is not computationally tractable, estimates of a tire's true contact area and shape must be provided to numerical models. Benchmarking, development, and validation of various numerical modeling approaches are currently planned for further internal investigation.

6.4 Best Practices and Lessons Learned: Empirical Models

When numerical or semi-empirical models are either impractical or insufficient for specific mobility scenarios, empirical testing can offer an alternative that captures the unique dynamics of ground contact interactions. Although empirical models may be quicker to develop and more cost-effective in certain cases, there are several best practices and considerations that should be adhered to when using these models for mobility simulations.

First, it is crucial to carefully design and carry out tests that reflect the conditions of the mobility scenario being modeled. Tests need to be representative of the operational environment, whether it involves traversing rocky terrain, soft soils, or a mixture of both. For instance, conducting single-wheel tests in appropriate soil simulants or on bedrock is essential to capture the complex tire-terrain interactions that can significantly affect mobility performance. The key factors, such as surface roughness, rock geometry, and the three-dimensional conformity of a tire around obstacles, must be considered to ensure that the empirical data generated reflects the real-world scenario as closely as possible.

Another important consideration is the considerable man-hours required to set up these types of experiments. Setting up realistic mobility tests often involves detailed planning, calibration, and data acquisition, which can be labor-intensive. For instance, generating look-up tables from single-component tests, such as tire deformation, friction, and thrust, requires substantial time and resources to collect meaningful data. These tests not only demand physical preparation but also involve rigorous post-processing to extract the parameters needed for system-level simulations.

Furthermore, one of the key limitations of empirical models is their inability to generalize across different mobility situations. While empirical relationships can be effective for the specific conditions under which the tests were conducted, they may not translate well to different environments. For example, data derived from soft soil traction tests may not be applicable to scenarios involving bedrock or rocky terrains. This challenge emphasizes the need to tailor empirical models to each distinct mobility scenario and underscores the importance of conducting a wide range of tests to cover various conditions.

In addition to these challenges, while empirical tests effectively capture input-output behavior for specific scenarios, they may offer limited insight into the physical mechanisms driving the observed behavior when test cases are not well-defined and

focused on specific mobility phenomena. Empirical approaches are data-driven from measurements of items under test, which, compared to other approaches presented in this paper, can more easily result in inaccurate or misleading models when variables that are not inherently correlated are fitted together, particularly when test cases lack well-defined boundaries or constraints. Although these models can replicate system performance under test conditions, they may fail to reveal the fundamental science behind tire-terrain interactions, material deformation, or multi-scale effects, leaving questions about the broader applicability of the results. This issue is exacerbated when only a few test cases are used to model complex behavior.

When used in a black-box manner, this lack of deeper understanding can also hinder the ability to extrapolate findings to new scenarios or adapt the model when key variables change. For example, an empirical model based on limited tests might accurately predict performance on one type of soil but fail when applied to a different terrain with different material properties. Therefore, while empirical testing is valuable, it should be complemented by other modeling techniques or broader testing to achieve a comprehensive understanding of the underlying physics.

In summary, empirical models offer a practical and efficient way to model ground contact interactions when other techniques may be infeasible. However, the success of these models hinges on rigorous and representative testing, significant preparation and effort, and an understanding of their limitations in generalizing to other mobility environments.

7 Ongoing Work

The preceding sections presented a range of tire–ground interaction modeling approaches, including those currently in use or under development at NASA Glenn Research Center, NASA Johnson Space Center, and the Jet Propulsion Laboratory. These methods span a wide spectrum of model fidelities, from relatively low-complexity, computationally efficient models to highly detailed, computationally intensive simulations. Each approach offers distinct advantages and limitations depending on the intended application, environmental context, and required accuracy.

Looking ahead, ongoing work aims to critically evaluate these modeling strategies with respect to their ability to capture relevant physical phenomena for off-world mobility simulations. A key objective is to systematically characterize what behaviors and mechanisms each modeling approach can represent and to document the associated trade-offs between fidelity and computational cost. This evaluation will inform the development of a multi-model framework that leverages the strengths of each method, enabling dynamic engagement of different models as needed to balance accuracy and efficiency across a range of mission-relevant scenarios.

To support this effort, several foundational capabilities are required to enable effective integration and evaluation of the modeling approaches, which is the focus of ongoing work. First, methods and test hardware for preparing regolith simulant test bins must be established to ensure repeatable and controlled conditions for data collection tasks, as this data is used for empirical validation and model calibration. Second, soil property parameters applied across modeling approaches must output

Figure 12. The DRAGON M Rig. (a) DRAGON M with soil bin filled with GRC-3B simulant. (b) Diagram of translational and rotational axes. Axis B, which mounts to the output of Axis A, not shown.

consistent results, requiring further research into model-specific parameter determination and calibration using experimental data. Third, development of a framework, potentially incorporating automated decision logic, is needed to select the most appropriate model or combination of models based on scenario-specific requirements, computational constraints, and the dominant physical mechanisms involved.

Ultimately, a long-term goal is to enable the use of computationally efficient models that retain the predictive power of more detailed simulations. To this end, future work will focus on extending the proposed multi-model framework by training surrogate models on high-fidelity simulation outputs. These data-driven approximations offer a promising pathway to reduce computational burden while preserving critical behavioral accuracy.

The following sections provide further detail on current development activities as well as planned future directions to advance the computational speed and fidelity of ground-contact models to increase their analytic capability and enable their use in both research and real-time systems.

7.1 Infrastructure for Soil Preparation and Mobility Testing

To enable consistent and repeatable terramechanics testing under simulated extraterrestrial conditions, the fully automated "Dynamic Regolith Assessment for Ground-Interaction with Objects and Novel Mechanisms (DRAGON M)" rig was developed (Fig. 12). This versatile system prepares and characterizes lunar regolith simulants in situ under tightly controlled laboratory conditions, supporting reproducible experiments for tool-soil interaction, wheel-soil contact force measurements, and excavation performance evaluation. With the capability to both loosen and compact the full depth of soil bins, DRAGON M achieves a broader range of soil

Table 3. DRAGON M Capabilities

Axis	Max Speed	Force/Torque Limit	Position Range/Resolution
X	5 m/s	1366 N	1850 mm ± 0.02 mm
Y	1 m/s	6146 N	850 mm ± 0.02 mm
Z	1 m/s	6146 N	850 mm ± 0.02 mm
A	600 rpm	109 N·m	Continuous ± 0.02°
B	57 rpm	48 N·m	Continuous ± 0.02°

states with greater accuracy than existing rigs. Additionally, it enables in situ characterization of soil via cone penetrometer, bevameter, and other geotechnical tool measurements, and facilitates testing of diverse articles including tires, rods, and blades.

DRAGON M is comprised of a rigid steel frame secured to the laboratory floor and encompasses a large soil bin filled with lunar regolith simulant. A dual-rail gantry spans the length of the bin and supports a vertical drive mast that traverses the bin's width and enables vertical motion. A motorized carriage on this mast enables controlled rotational speed for various tool attachments. The device provides five degrees of motion: three translational axes (X, Y, Z) and two rotational axes (A, B), all servo-driven with precision control (Fig. 12b).

Interchangeable tool attachments include a 101.6 mm-diameter auger, a 60-degree cone penetrometer, and a wheel-soil interaction assembly. Tools are mounted on a lathe chuck for rotation about the vertical axis (A-axis). A mobility testing assembly, featuring a 6-axis load cell and horizontal axle (B-Axis), can be mounted to the chuck to evaluate wheel performance under various soil conditions.

The B-axis load cell measures up to 1 kN in the lateral (F_y) direction, 4 kN in the lateral (F_x) and vertical (F_z) directions, and torques (M_x, M_y, M_z) up to 250 N·m. A string potentiometer on the Z-carriage records vertical displacement during sinkage and penetration testing. Motion control is provided by ELMO servo drives powered from a 208 VAC, three-phase supply converted to 325 VDC. Multi-turn absolute encoders on each axis enable sub-millimeter precision. All motion and data acquisition are handled via a custom LabVIEW interface, which enables real-time control of position, velocity, and tool forces.

To evaluate the consistency of automated soil preparation using DRAGON M, a series of soil loosening trials were conducted using the auger tool. The auger used features a 101.6 mm diameter, a 67.73 mm pitch, and a 609.6 mm bladed length. Drilling was performed with an insertion angular velocity of 400°/s and a withdrawal speed of -360°/s, at a linear feed rate of 68 mm/s. The rotational motion was programmed with an acceleration of 500°/s^2 and a jerk of 2000°/s^3. A total of 96 auger holes were distributed evenly across the bin surface to uniformly loosen the soil. Following augering, the surface was manually leveled using a wooden drag implement to ensure a smooth, flat surface for subsequent testing.

Soil mechanical properties were measured using cone penetrometer tests. Cone penetrometer testing is a geotechnical characterization technique in which a conical

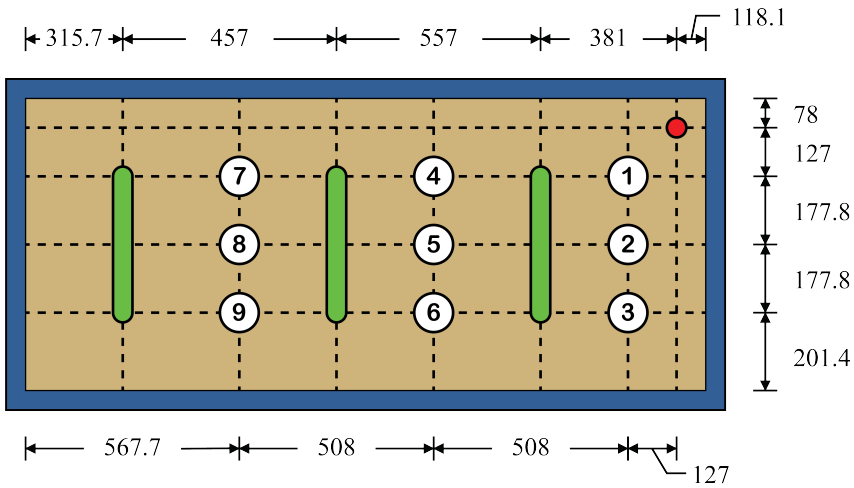

Figure 13. Cone penetrometer and cylindrical probe drag test locations. Red dot: Origin. Numbered Circles: Locations of cone penetrometer tests. Green cylinder: cylindrical probe drag test region. All dimensions are in mm.

probe is driven into soil at a constant rate to measure tip resistance and sleeve friction, which relate to soil strength and stiffness properties [28].

A 60° cone with a 500 mm^2 base area was mounted in DRAGON M to conduct penetration tests at nine distinct locations throughout the soil bin (Fig. 13). Test sites were selected to characterize both central and peripheral regions of the bin, providing insights into spatial variability and potential boundary effects. Test locations were also spaced to allow for drag testing with a cylindrical probe, enabling the development and validation of simulation models using a single, consistently prepared soil volume. [2]

Tip resistance versus depth for four soil preparation trials is shown in Figure 14, along with trial means and standard deviations. Mean tip resistance at each test location versus depth is shown in Figure 15 to enable easier comparison of variability between test locations. The depth range of 0–200 mm was selected to reflect typical wheel sinkage depths expected during mobility testing. The results show high consistency in tip resistance values, particularly between 0–100 mm, indicating uniform soil loosening and compaction in this zone. Increased variability was observed at depths greater than 100 mm, which may reflect the limit of auger penetration effectiveness or variations in soil re-consolidation at depth. Importantly, no significant edge effects were observed when comparing central and peripheral test locations.

To further assess consistency, the cone index gradient was computed as the rate of change of tip resistance with respect to depth, evaluated in 50 mm increments between 0 and 200 mm. Cone index gradient represents the rate of change of resistance with depth and serves as a proxy for stiffness stratification in prepared soil beds. It is calculated by numerically differentiating force-depth curves. As shown in Figure

[2]Capturing both drag test data and cone penetrometer measurements from the same soil preparation supports future model tuning and validation tasks, though this work is beyond the scope of this paper.

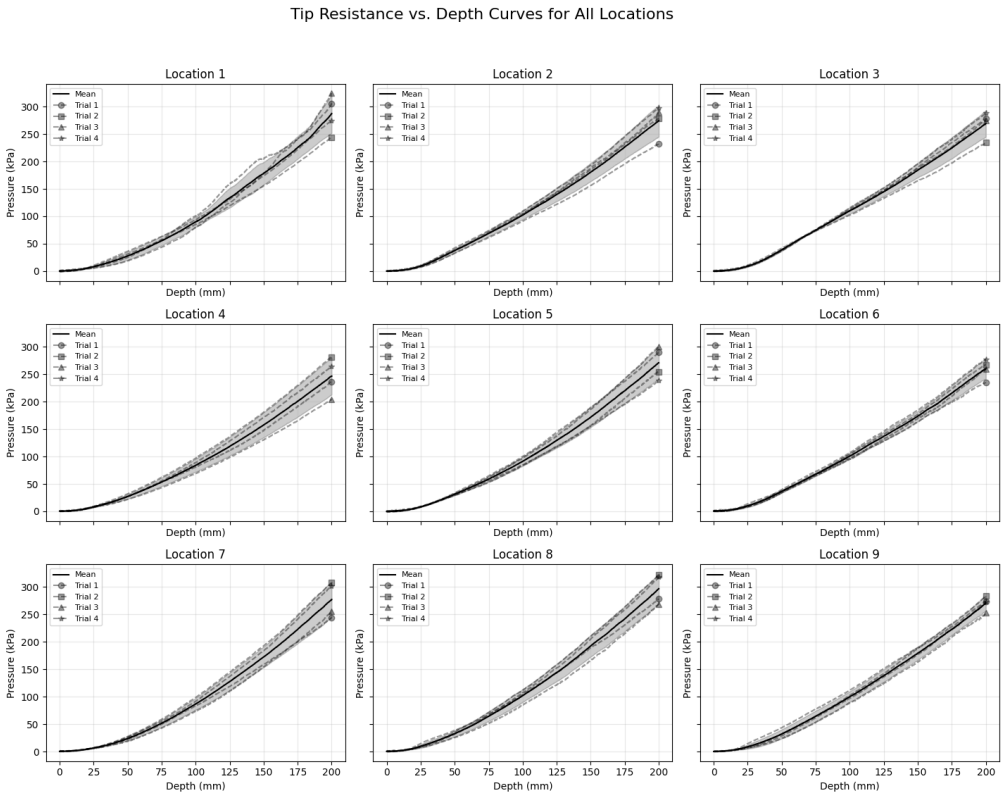

Figure 14. Cone penetrometer tip resistance vs. depth for four soil preparation trials.

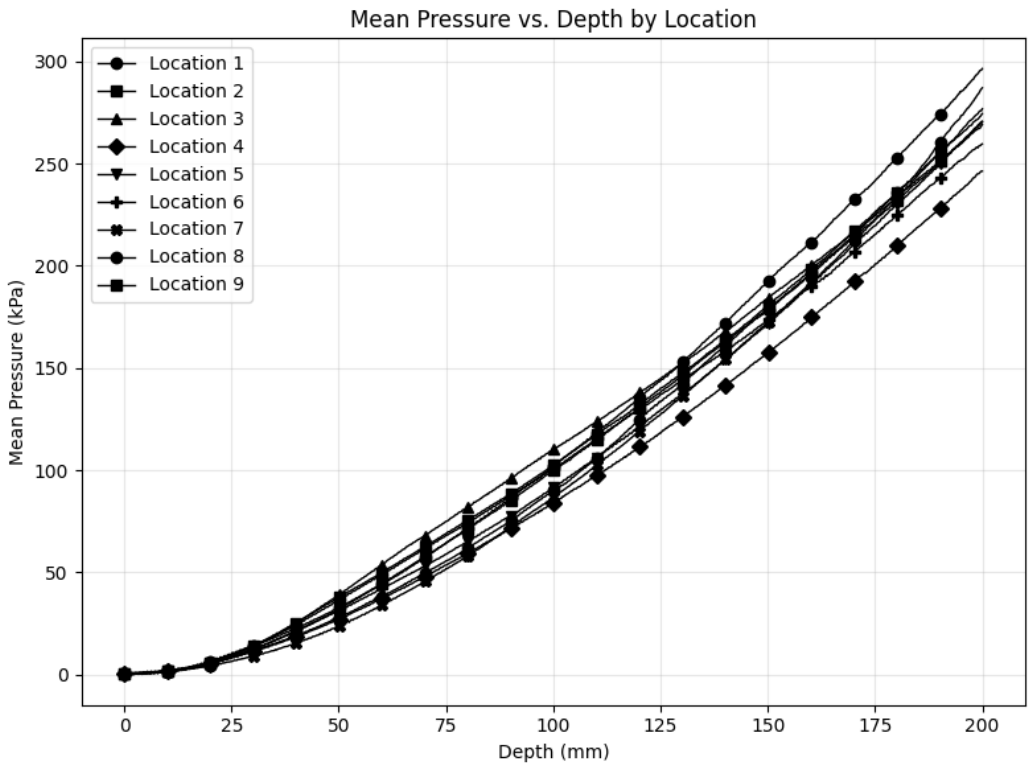

Figure 15. Mean cone penetrometer tip resistance vs. depth at all test locations.

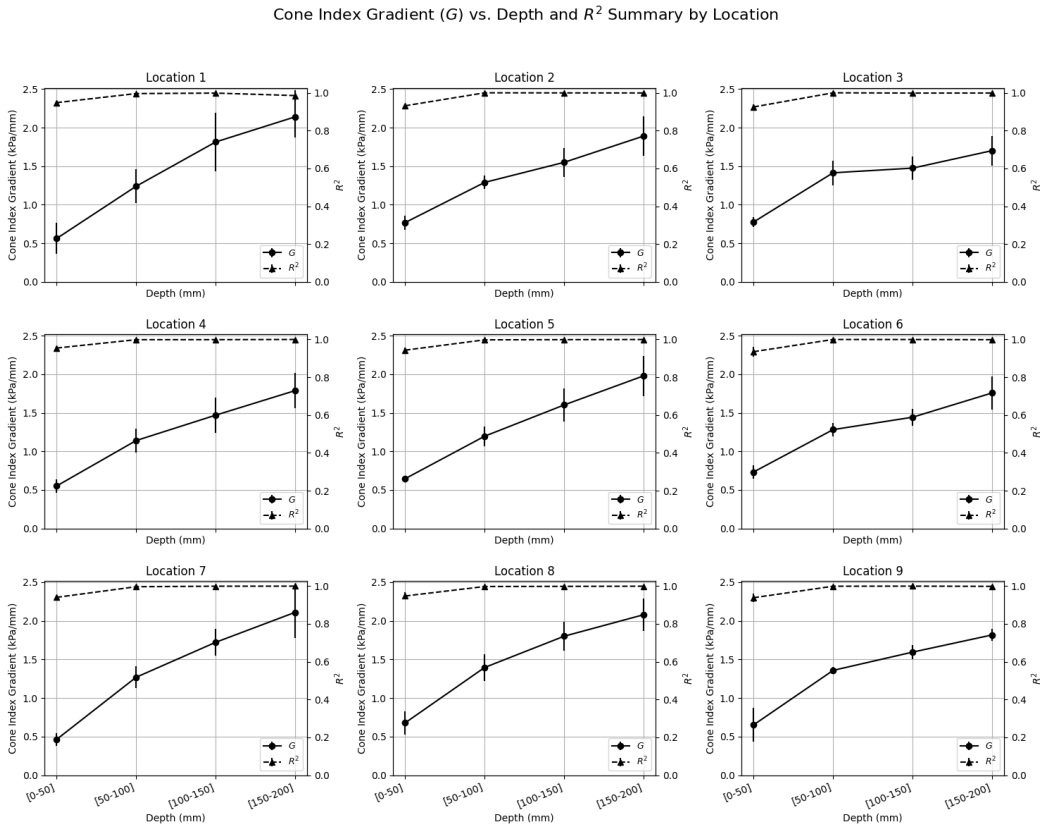

Figure 16. Averaged cone index gradient (G) vs. depth at test locations 1 to 9.

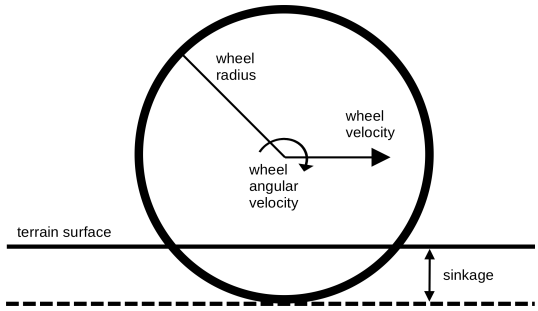

Figure 17. Diagram of simulated drawbar pull tests.

16, tip resistance increases with depth in all trials, consistent with expectations for loose topsoil overlaying more compact subsurface material.[3] The high correlation between cone index profiles at each location and across trials reinforces the conclusion that DRAGON M produces a repeatable soil state, particularly within the top 100 mm of the prepared bed.

7.2 Ongoing Development and Assessment of Modeling Approaches

To support mobility analysis and inform simulation tool development, a parallel effort was initiated to compare modeling approaches for wheel–soft-soil interaction. This study evaluates the capabilities, limitations, and trade-offs of two existing simulation frameworks by modeling a standard single-wheel drawbar pull test (Fig. 17). Key performance metrics, such as sinkage, slip, drawbar pull force, and computation time, are used to assess both model fidelity and runtime efficiency. The results serve as a foundation for a broader evaluation of wheel–terrain interaction simulation methods. Ultimately, soil property data generated through the automated soil preparation and characterization process described previously will be used to calibrate and validate these models, ensuring that simulations are grounded in experimentally derived parameters.

Five terramechanics models were chosen to capture a broad range of capability and performance that would be suitable for mobility studies from faster-than-real-time traverse analysis to offline design analysis. DARTS [20, 16] and Chrono [34] were chosen for this comparison as these two simulation environments together support terramechanics models that cover the entire spectrum of models discussed in this paper. DARTS is an ecosystem for physics-based modeling and simulation for planetary exploration, supporting closed-loop and offline analysis of orbiters, landers, rovers, rotorcraft, and robotic platforms. It is a tool developed at the Jet Propulsion Laboratory (JPL) in support of flight projects and research and development. Chrono is an open-source, physics-based simulation framework for vehicle, robot, and mechatronic systems, including closed-loop and offline analysis of vehicle mobility and vehicle-terrain interaction.

[3]Calculated mean cone index gradient values and associated mean correlation coefficients for each location at each depth are provided in the Appendix.

Table 4. Real-time factor (RTF) comparison. Evaluated methods span a wide range of speeds. (RTF < 1 is faster than real time.)

Method	**Real-Time Factor (RTF)**	**Simulated Terrain Length**
DARTS-Bekker	0.024	Analytical plane
Chrono-SCM	0.41	19 m with 1.67 cm resolution
Chrono-CRM	47	5 m with 4.4×10^5 markers
Chrono-DEM	9600	2 m with 1.1×10^6 particles

In this ongoing effort, DARTS is used to evaluate the implementation of an idealized Bekker model (see Sec. 3.1) whose implementations are designed to support analysis of long traverses that can be simulated much faster than real time. To compare higher-fidelity models, Chrono is used to evaluate a more geometrically detailed Bekker-Wong model: Soil Contact Model (SCM) [32] (Sec. 3.1), and two physics-based models: a continuum representation model (CRM) [15] (Sec. 4.0.2) and a discrete element model (DEM) [41] (Sec. 4.0.3). These approaches are designed to more completely capture the interaction between the wheel and soil but are more computationally intensive.

To stand up a preliminary comparison across different simulations, parameters from literature, specifically a consistent set used for modeling GRC-1 under Earth gravity, are applied. These parameters are sourced from various publications and are therefore not guaranteed to be consistent across different types of models. Instead, they represent a first pass to provide consistency of GRC-1 parameters from various sources for a given model. However, a fully calibrated and consistent set of model parameters is not yet available for this initial comparison and will be the focus of future work using the capabilities of DRAGON M. Parameters for DARTS-Bekker and Chrono-SCM where obtained from Hu et al. [15]. The CRM parameters were obtained from the same paper and its associated reproducibility scripts. Chrono-DEM parameters were obtained through available Chrono-GPU and Chrono DEM-Engine demos [41]. For this comparison, each simulation models a rigid cylindrical grouserless wheel with radius of 0.25 m and width of 0.2 m.

While improved calibration of these model parameters and validation against the soil test bed experimentation is future work, the results from this preliminary effort can be used to begin to tease out the qualitative trade-offs between the approaches. Specifically, trends in the results can be used to elucidate regimes where models are expected to have limiting assumptions that result in unmodeled physics dominating the mobility characteristics.

There is a theoretical trade-off between how faithfully and completely terramechanics models capture wheel-terrain interaction and the computational complexity of these models. To demonstrate the computational time, the virtual single-wheel test was run with each method on the same engineering workstation, capturing the run-time of the simulation. The results, shown in Table 4, indicate the real-time factor (RTF) for the single wheel test using each of the five methods. The test machine was a workstation with an Intel i9-13900K Central Processing Unit (CPU) and

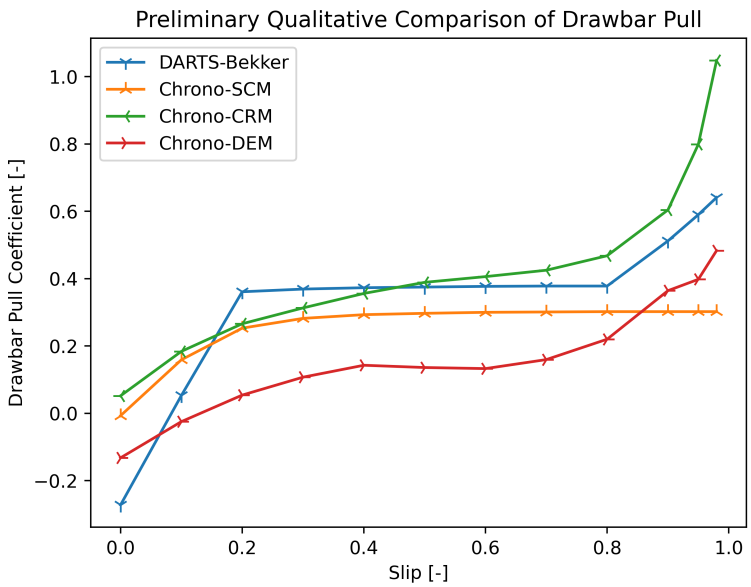

Figure 18. Comparison of drawbar pull coefficient demonstrates some of the behavior that differentiates the methods.

a NVIDIA RTX 4090 Graphics Processing Unit (GPU). Note that DARTS-Bekker and Chrono-SCM are CPU-only whereas Chrono-CRM and Chrono-DEM are GPU implementations.

The methods are listed in order of increasing fidelity, with DARTS-Bekker relying on the most constraining assumptions, and Chrono-DEM representing the most physically-complete description of the system. As expected, with each step of increased fidelity/complexity comes increased compute time. These results begin to demonstrate where each model could be leveraged: which models could be used for long-duration traverse analysis and those that may be restricted to detailed, short-duration mobility studies.

While one aspect of the trade-off is compute time, it is important to understand the limitations of the computationally efficient models and how those limitations impact the modeled phenomena. The single-wheel drawbar pull test demonstrates this qualitatively, with future work to calibrate the simulations and perform quantitative comparison. Sinkage and drawbar pull force for each of the four simulations were collected for slip from 0.0 to 0.98. Qualitatively, models should generate slip and drawbar pull forces similar to those shown in Figure 1. Simulated results showing drawbar pull coefficient versus slip are shown in Figure 18. Sinkage versus slip is shown in Figure 19.

The first regime of interest where the methods exhibit significantly different behavior is at high slip where theoretical assumptions of Bekker-Wong are limiting. In this high-slip regime, material is displaced from beneath the wheel, no longer following a Bekker-Wong soil stress characterization. Because of this, DARTS-Bekker and Chrono-SCM are unable to fully capture the effect of material being excavated

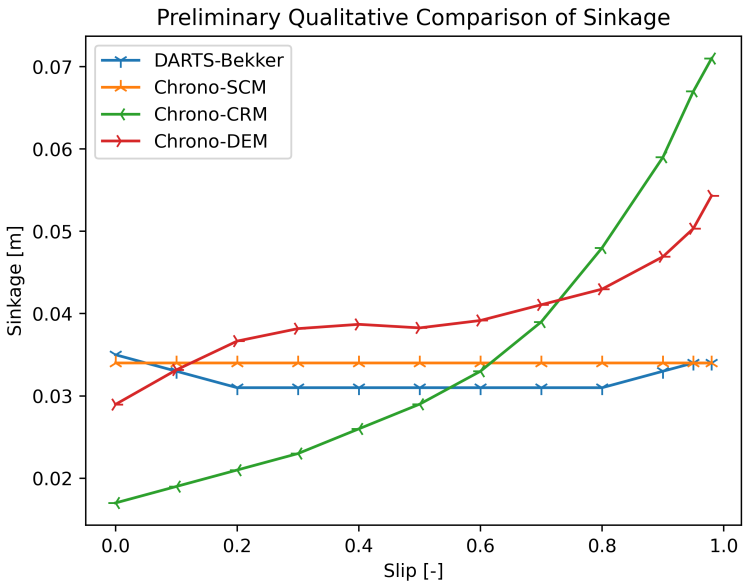

Figure 19. Sinkage vs. slip. Only CRM and DEM capture increased regolith displacement with slip.

on sinkage or drawbar pull force, which is most evident in Figure 19 where DARTS-Bekker, and Chrono-SCM show near constant sinkage. However, Chrono-CRM, and Chrono-DEM all demonstrate the strong correlation between sinkage and slip. This difference is also realized in drawbar pull force, shown in Figure 18, where the approaches that capture the displacement of soil also capture a sharp increase in drawbar pull force as slip approaches 1.0. It should be noted that due to discrepancies between soil parameters used for different models, the ability to accurately capture dynamics for each method should not be inferred from these results. These preliminary tests are only meant to assess the ability of each type of simulation to capture various qualitative phenomena. Refinement of both the underlying single wheel simulation and model parameters is ongoing and the subject of future work.

Evident in Figure 18 is a second regime of interest even for this simple, single-wheel test: very low slip. DARTS-Bekker exhibits a much sharper increase in drawbar pull force between 0.0 and 0.2 slip and has much lower drawbar pull force at zero slip than Chrono-SCM, whose theory closely matches DARTS-Bekker. One explanation for this is that DARTS-Bekker ignores geometric effects of the terrain deformation, resulting in a less-precisely modeled contact patch, and less-precisely modeled relative motion between the wheel and soil. However, this simplification results in faster evaluation time (see Table 4).

While further work is needed to more precisely and comprehensively calibrate and compare these models, each approach demonstrates a clear trade-off between fidelity and performance that can help indicate where each approach could best be leveraged.

Table 5. Comparison of modeling approaches for wheel-terrain interaction: advantages, drawbacks, and knowledge gaps.

Modeling Approach	**Advantages**	**Drawbacks**	**Gaps / Limitations**
Classical Terramechanics (Semi-Empirical)	• Computationally efficient • Suitable for real-time and human-in-the-loop simulations • Generalizable across similar terrains	• Lower fidelity than numerical or empirical models • Limited in complex terrain or with compliant wheels	• Cannot capture high-deformation or nonlinear material behavior • Insufficient for modeling compliant or mesh tires
Numerical Methods (FEM, SPH, DEM)	• High fidelity modeling of complex interactions • Capable of simulating compliant tires, 3D deformations, and particle-soil dynamics • Supports sensitivity studies and design iteration reduction	• Computationally intensive • Often unsuitable for real-time use • Require significant input data and parameter tuning	• Accurate tire-soil interface modeling is still underdeveloped • Friction calibration and validation data are scarce • DEM particle simplifications reduce realism
Empirical Approaches	• Captures full-system behavior in specific mobility conditions • Suitable for rapid prototyping and real-time simulations • Useful where numerical modeling is infeasible	• Limited generalizability • Cannot extrapolate to new scenarios without re-testing	• Often require extensive testing to build datasets • Cannot resolve internal mechanisms or physics-based insight

8 Conclusion and Future Work

This paper has outlined a range of modeling approaches for tire-ground contact, highlighting ongoing developments at NASA Glenn Research Center, NASA Johnson Space Center, the Jet Propulsion laboratory, and the broader modeling landscape. Each method presents a trade-off between physical accuracy and computational efficiency, with different strengths depending on the application and operating environment. For convenience, the advantages, drawbacks, and gaps/limitations of each discussed approach is presented in Table 5. To move toward a robust modeling framework suitable for the next generation of lunar and martian mobility systems, continued testing, validation, and model refinement are essential.

Immediate work is focused on advancing in-house high-fidelity simulation tools by calibrating models with soil parameters derived from experimental data collected in simulant soil bins. This calibration uses numerical optimization techniques to tune soil properties in Chrono simulations to match observed behavior. While this approach significantly enhances the predictive capability of high-fidelity models, it is time-intensive and not scalable across many terrain types or mission scenarios.

To address this, near-term work will focus on exploring faster and more practical calibration methods that reduce reliance on full optimization cycles. Establishing consistency in soil parameters across models of varying fidelity, ranging from high-fidelity particle-based simulations to real-time-capable empirical models, is a key goal. Consistent parameterization will enable confidence in the accuracy of different modeling methods when applied to the same mobility scenario, regardless of computational constraints. These efforts will be supported by upcoming test campaigns leveraging the newly developed DRAGON M rig, which enables consistent soil preparation for data collection. Example approaches include using cone penetrometer data to estimate soil strength parameters, as well as applying numerical optimization techniques to tune models based on empirical data from test articles traversing the prepared soil. Both methods can be used for model calibration and performance assessment. Additional techniques may also be explored as the modeling framework evolves.

In parallel, efforts will explore the integration of uncertainty quantification frameworks to support dynamic model selection. Such frameworks could guide when lower-fidelity models are sufficient and when high-fidelity "child" simulations should be spawned to resolve key uncertainties or nonlinear interactions. This hybrid modeling approach offers a practical path to balance physical realism with computational efficiency.

Surrogate modeling represents another promising direction. While particle-based simulation methods like DEM continue to improve, their large computational costs currently limits their use for real-time applications. However, high-fidelity simulations can serve as training data for machine-learning-based surrogate models that accurately estimate forces and torques from system state variables. Such surrogate models could retain the predictive power of detailed physics-based methods while enabling real-time inference on resource-constrained systems.

Finally, the strategies of faster calibration, adaptive hybrid modeling, and surrogate model development, lay the foundation for more complex and realistic sim-

ulations. By reducing computational burdens, it becomes feasible to incorporate additional effects such as wheel compliance and soil heterogeneity. This enables broader support for digital engineering workflows, including simulation-based design optimization and system-level trade studies for extreme terrain mobility.

In the long term, the goal is to develop a suite of scalable, high-fidelity, and computationally efficient modeling tools that support robust, long-duration simulations of compliant tire systems operating in planetary environments. These tools must be adaptable to the needs of rover developers, which will be informed through continued engagement with the community. The resulting simulation environments will support not only engineering design but also fundamental research into mobility performance and terrain interaction, advancing the capabilities of exploration systems for the Moon, Mars, and beyond.

Appendix A

Additional Tables

Table A1. Mean Cone Index Gradient and R^2 Values for DRAGON M Automated Soil Preparation Experiments.

Location	**Depth Range (mm)**	**Mean Cone Index Gradient**	**Mean R^2**
1	0 - 50	0.5618 ± 0.2013	0.9475 ± 0.0093
	50 - 100	1.2396 ± 0.2176	0.9955 ± 0.0040
	100 - 150	1.8138 ± 0.3765	0.9981 ± 0.0015
	150 - 200	2.1397 ± 0.2673	0.9849 ± 0.0266
2	0 - 50	0.7684 ± 0.0925	0.9310 ± 0.0092
	50 - 100	1.2892 ± 0.0869	0.9994 ± 0.0003
	100 - 150	1.5498 ± 0.1853	0.9989 ± 0.0006
	150 - 200	1.8906 ± 0.2559	0.9987 ± 0.0015
3	0 - 50	0.7758 ± 0.0677	0.9247 ± 0.0121
	50 - 100	1.4142 ± 0.1606	0.9995 ± 0.0002
	100 - 150	1.4748 ± 0.1500	0.9981 ± 0.0016
	150 - 200	1.7016 ± 0.1913	0.9984 ± 0.0016
4	0 - 50	0.5511 ± 0.0877	0.9540 ± 0.0106
	50 - 100	1.1403 ± 0.1569	0.9983 ± 0.0007
	100 - 150	1.4695 ± 0.2252	0.9984 ± 0.0013
	150 - 200	1.7879 ± 0.2317	0.9994 ± 0.0001
5	0 - 50	0.6453 ± 0.0408	0.9427 ± 0.0126
	50 - 100	1.1964 ± 0.1286	0.9974 ± 0.0026
	100 - 150	1.6018 ± 0.2165	0.9984 ± 0.0010
	150 - 200	1.9794 ± 0.2611	0.9992 ± 0.0004
6	0 - 50	0.7325 ± 0.0863	0.9348 ± 0.0262
	50 - 100	1.2820 ± 0.0883	0.9993 ± 0.0002
	100 - 150	1.4430 ± 0.1072	0.9992 ± 0.0005
	150 - 200	1.7578 ± 0.2134	0.9982 ± 0.0017
7	0 - 50	0.4629 ± 0.0803	0.9400 ± 0.0059
	50 - 100	1.2691 ± 0.1393	0.9961 ± 0.0007
	100 - 150	1.7222 ± 0.1753	0.9989 ± 0.0013
	150 - 200	2.1112 ± 0.3303	0.9992 ± 0.0005
8	0 - 50	0.6773 ± 0.1532	0.9471 ± 0.0188
	50 - 100	1.3957 ± 0.1716	0.9972 ± 0.0015
	100 - 150	1.8012 ± 0.1860	0.9980 ± 0.0009
	150 - 200	2.0801 ± 0.2102	0.9989 ± 0.0003
9	0 - 50	0.6513 ± 0.2174	0.9380 ± 0.0220
	50 - 100	1.3581 ± 0.0443	0.9988 ± 0.0010
	100 - 150	1.5950 ± 0.0884	0.9992 ± 0.0005
	150 - 200	1.8179 ± 0.0809	0.9981 ± 0.0006

References

[1] S Agarwal et al. "Modeling of the interaction of rigid wheels with dry granular media". In: *Journal of Terramechanics* 85 (2019), pp. 1–14.

[2] V Asnani, D Delap, and C Creager. "The development of wheels for the Lunar Roving Vehicle". In: *Journal of Terramechanics* 46.3 (2009), pp. 89–103.

[3] MG Bekker. "Land locomotion on the surface of planets". In: *ARS journal* 32.11 (1962), pp. 1651–1659.

[4] MG Bekker. "Off-Road Locomotion". In: *Ordnance* 53.292 (1969), pp. 416–418.

[5] R Bernstein. "Problems of the experimental mechanics of motor ploughs". In: *Der Motorwagen* 16 (1913).

[6] W David Carrier III. *Lunar soil simulation and trafficability parameters*. Lunar Geotechnical Institute, 2006.

[7] CM Creager et al. "Best Practices for the Testing of Planetary Roving Vehicle Mobility Systems and Tires". In: *NASA White Paper NASA/WP-20250003470* (2025).

[8] PA Cundall and ODL Strack. "A discrete numerical model for granular assemblies". In: *Geotechnique* 29.1 (1979), pp. 47–65.

[9] DL Dewhirst. "A load-sinkage equation for lunar soils". In: *AIAA Journal* 2.4 (1964), pp. 761–762.

[10] DR Freitag et al. "Wheels for lunar vehicles". In: *Journal of Terramechanics* 8.3 (1972), pp. 89–105.

[11] BP Goriatchkin. "Theory and manufacturing of agricultural machines". In: *Moscow, USSR Goverment* (1936).

[12] R He et al. "Review of terramechanics models and their applicability to real-time applications". In: *Journal of Terramechanics* 81 (2019), pp. 3–22.

[13] C Holm, GJ Hefer, and D Hinze. "The influence of shape and size of a penetration body on the pressure sinkage relationship". In: *Proceedings of the 9th International ISTVS Conference, Barcelona, Spain*. Vol. 31. 1987, pp. 28–36.

[14] MA Hopkins, JB Johnson, and R Sullivan. "Discrete element modeling of a rover wheel in granular material under the influence of Earth, Mars, and Lunar Gravity". In: *Earth & Space 2008: Engineering, Science, Construction, and Operations in Challenging Environments*. 2008, pp. 1–7.

[15] W Hu et al. "Calibration of an expeditious terramechanics model using a higher-fidelity model, Bayesian inference, and a virtual bevameter test". In: *Journal of Field Robotics* 41.3 (2024), pp. 550–569.

[16] A Jain et al. “Roams: Planetary surface rover simulation environment”. In: (2003).

[17] Z Janosi and B Hanamoto. “An analysis of the drawbar pull vs slip relationship for track laying vehicles”. In: (1961).

[18] JB Johnson et al. “Discrete element method simulations of Mars Exploration Rover wheel performance”. In: *Journal of Terramechanics* 62 (2015), pp. 31–40.

[19] W Li et al. “Trafficability analysis of lunar mare terrain by means of the discrete element method for wheeled rover locomotion”. In: *Journal of Terramechanics* 47.3 (2010), pp. 161–172.

[20] Christopher S Lim and Abhinandan Jain. “Dshell++: A component based, reusable space system simulation framework”. In: *2009 Third IEEE International Conference on Space Mission Challenges for Information Technology*. IEEE. 2009, pp. 229–236.

[21] E McKyes and T Fan. “Multiplate penetration tests to determine soil stiffness moduli”. In: *Journal of Terramechanics* 22.3 (1985), pp. 157–162.

[22] P Naghipour, L Aktay, and AF Johnson. “Numerical investigation of structural crash response of thin-walled structures on soft soil”. In: *Materials & Design* 29.10 (2008), pp. 2052–2060.

[23] P Naghipour et al. “Development and Implementation of Large-Scale Numerical Models for Shape Memory Mars Spring Tires”. In: *NASA Technical Memorandum* NASA/TM-20230009408 (2024).

[24] H Nakashima et al. “Discrete element method analysis of single wheel performance for a small lunar rover on sloped terrain”. In: *Journal of Terramechanics* 47.5 (2010), pp. 307–321.

[25] HA Oravec. *Understanding mechanical behavior of lunar soils for the study of vehicle mobility*. Case Western Reserve University, 2009.

[26] S Papamichael and C Vrettos. “Indentation tests and rolling simulations of a compliant wheel on soil at different consistencies”. In: *Journal of Terramechanics* 94 (2021), pp. 39–48.

[27] Alan R Reece and Land Locomotion Laboratory (US). *Problems of soil vehicle mechanics*. Army Tank-Automotive Center, 1964.

[28] JD Rogers. “Fundamentals of cone penetrometer test (CPT) soundings”. In: *Missouri University of Science and Technology* (2020).

[29] D Rubinstein, I Smulevich, and NF Technion. “Use of explicit finite-element formulation to predict the rolling radius and slip of an agricultural tire during travel over loose soil”. In: *Journal of Terramechanics* (2019).

[30] Z El-Sayegh et al. “Improved tire-soil interaction model using FEA-SPH simulation”. In: *Journal of Terramechanics* (2018).

[31] AD Sela and IR Ehrlich. “Load support capability of flat plates of various shapes in soils”. In: *Journal of terramechanics* 8.3 (1972), pp. 39–69.

[32] R Serban, J Taves, and Z Zhou. "Real-time simulation of ground vehicles on deformable terrain". In: *Journal of Computational and Nonlinear Dynamics* 18.8 (2023), p. 081007.

[33] SA Shoop. *Finite element modeling of tire-terrain interaction*. University of Michigan, 2001.

[34] A Tasora et al. "Chrono: An open source multi-physics dynamics engine". In: *High Performance Computing in Science and Engineering: Second International Conference, HPCSE 2015, Soláň, Czech Republic, May 25-28, 2015, Revised Selected Papers 2*. Springer. 2016, pp. 19–49.

[35] FA Tavarez and ME Plesha. "Discrete element method for modelling solid and particulate materials". In: *International journal for numerical methods in engineering* 70.4 (2007), pp. 379–404.

[36] JY Wong. "Data processing methodology in the characterization of the mechanical properties of terrain". In: *Journal of Terramechanics* 17.1 (1980), pp. 13–41.

[37] JY Wong. *Theory of ground vehicles*. John Wiley & Sons, 2001.

[38] JY Wong and W Huang. ""Wheels vs. tracks"–A fundamental evaluation from the traction perspective". In: *Journal of Terramechanics* 43.1 (2006), pp. 27–42.

[39] JY Wong and AR Reece. "Prediction of rigid wheel performance based on the analysis of soil-wheel stresses part I. Performance of driven rigid wheels". In: *Journal of Terramechanics* 4.1 (1967), pp. 81–98.

[40] R Zhang et al. "A GPU-accelerated simulator for the DEM analysis of granular systems composed of clump-shaped elements". In: *Engineering with Computers* (2024), pp. 1–21.

[41] R Zhang et al. "Chrono DEM-Engine: A Discrete Element Method dual-GPU simulator with customizable contact forces and element shape". In: *Computer Physics Communications* 300 (2024), pp. 109–196.